Near-Field Characterization of a Free Space Channel Model for Ultra Wideband Radio

Sathaporn Promwong[†], Pichaya Supanakoon[†], Monchai Chamchoy[†], Sompoph Keawmechai[†], and Jun-ichi Takada[††]

[†]Department of Information Engineering, Faculty of Engineering,
King Mongkut's Institute of Technology Ladkrabang, Bangkok 10520, Thailand.
E-mail: kpsathap@kmitl.ac.th

[††]Graduate School of Science and Engineering, Tokyo Institute of Technology
O-okayama Minami 6 Bldg., 2-12-1, O-okayama, Meguro-ku, Tokyo 152-8550, Japan.
E-mail:takada@ap.ide.titech.ac.jp

Abstract

Friis' transmission formula in complex form to treat the UWB signals to take into account the waveform distortion due to the frequency characteristics of the antennas [1], [2]. It is noted that Friis' transmission formula is applicable only in the far field region. In personal area network (PAN) environments, however, the distance may not satisfy the far field condition. In this paper, we discusses the experimental evaluation of the transmission properties in Fresnel region.

Keywords: UWB-IR, UWB antennas, UWB measurements, Friis' transmission formula, Three-antenna method

1. Introduction

The ultra wideband impulse radio (UWB-IR) transmission systems have attracted a great deal of attention because of its potentiality for application to short-range, high-speed mobile communications, low-power transmission, and so on. In order to minimize the interference with existent systems, the UWB is expected to be used mainly in wireless personal area networks (WPANs) and home networks.

The channel in line of sight (LOS), Friis' transmission formula cannot be directly applied to the UWB radio as the bandwidth of the pulse is extremely wide. Furthermore, simple comparison between waveforms of the transmitter and the receiver is not significant because of the distortion of the waveform caused by the frequency response of the antenna.

In this paper, the experimental results of the transmission properties in Fresnel region.

2. Friis' Formula for UWB System

The Friis' transmission formula is first expressed in terms of power [2]. Then it is extended in terms of the transmission signal waveform to consider the transfer function H_{Friis} [2]. Defining the transmitted and received voltage signals as V_{r} and V_{t}, respectively, and assuming the polarization of transmitter and receiver antennas match perfectly.

We obtain

$$H_{\mathrm{Friis}}(f,d) = \frac{V_{\mathrm{r}}(f)}{V_{\mathrm{t}}(f,d)} = H_{\mathrm{f}}(f,d)H_{\mathrm{r}}(f)H_{\mathrm{t}}(f), \quad (1)$$

where H_{f} is the transfer function of free space, H_{r} and H_{t} are the transfer functions of the transmitting (Tx) and the receiving (Rx) antennas, which are implicit functions of directions, and d is the transmitter-receiver (TR) separation distance.

The transfer function of free space can be written as

$$H_{\mathrm{f}} = \frac{\lambda}{4\pi d}\exp(-\mathrm{jkd}), \quad (2)$$

is the free space transfer function where

$$k = \frac{2\pi}{\lambda} \quad (3)$$

is the propagation constant. The received waveform $v_{\mathrm{r}}(t,d)$ can be found by using

$$v_{\mathrm{r}}(t,d) = v_{\mathrm{t}}(t) \otimes h_{\mathrm{Friis}}(t,d), \quad (4)$$

where $v_{\mathrm{t}}(t)$ is the transmitted signal waveform, $\otimes$ is the convolution operator, $h_{\mathrm{Friis}}(t,d)$ is the impulse response of the extension of Friis' formula defined as:

$$h_{\mathrm{Friis}}(t,d) = \mathcal{F}^{-1}\{H_{\mathrm{Friis}}(f,d)\}, \quad (5)$$

where $\mathcal{F}^{-\infty}\{\cdot\}$ is the inverse Fourier transform.

3. UWB Transfer Function Measurement

3.1 Measurement Scheme

The complex transfer functions can be measured by using the vector network analyzer (VNA). However, this transfer function is a product of transfer functions of Tx and Rx antennas as well as the free space channel. The transfer function of the Tx antenna, which is usually a standard antenna, shall be known in advance as the calibration data. The overall measurement scheme is summarized as follows:

Step 1) Calibration of the standard antenna. The standard antenna is calibrated by using the three-antenna method. In this method, three linearly-polarized antennas are required, but they do not have

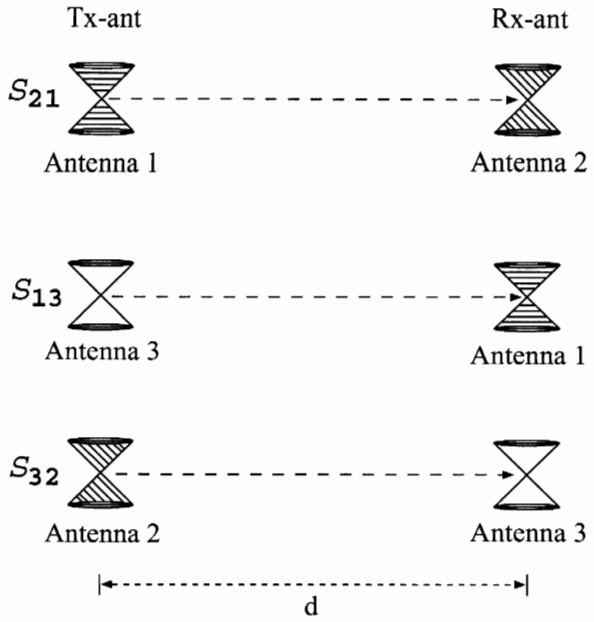

Fig. 1. Three antenna model.

to be identical to one another. Three sets of measurements are performed using all combinations of the three antennas pointing toward the same directions as shown in Fig. 1. The result is a set of three simultaneous equations of the form

$$S_{21}(f) = H_1(f)H_f(f,d)H_2(f), \quad (6)$$
$$S_{13}(f) = H_3(f)H_f(f,d)H_1(f), \quad (7)$$
$$S_{32}(f) = H_2(f)H_f(f,d)H_3(f), \quad (8)$$

where $H_i(f)$ is the complex frequency transfer function of antenna i, S_{ji} is the measurement result by using Tx antenna i and Rx antenna j, d is the distance between antennas, and $H_f(f,d)$ is the complex transfer function of free space. Then, we can estimate the complex frequency transfer function of the antennas by using these equations

$$H_1(f) = \sqrt{\frac{S_{21}(f)S_{32}(f)}{S_{13}(f)H_f(f,d)}}, \quad (9)$$

$$H_2(f) = \sqrt{\frac{S_{21}(f)S_{13}(f)}{S_{32}(f)H_f(f,d)}}, \quad (10)$$

$$H_3(f) = \sqrt{\frac{S_{32}(f)S_{13}(f)}{S_{21}(f)H_f(f,d)}}. \quad (11)$$

Step 2) The transfer function of the antenna under teat (AUT) is measured. By using the standard antenna and the AUT as Tx and Rx antennas respectively, the transfer function between Tx and Rx antenna ports is expressed as

$$S_{21}(f) = H_{AUT}(\theta,\varphi,f)H_f(f,d)H_{Std}(f), \quad (12)$$

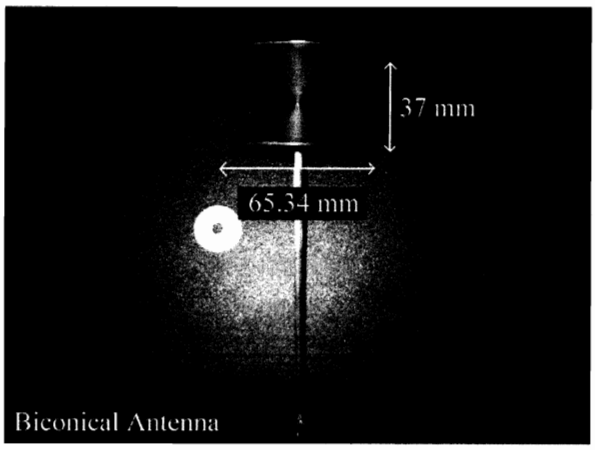

Fig. 2. Geometry and dimensions of the biconical antenna.

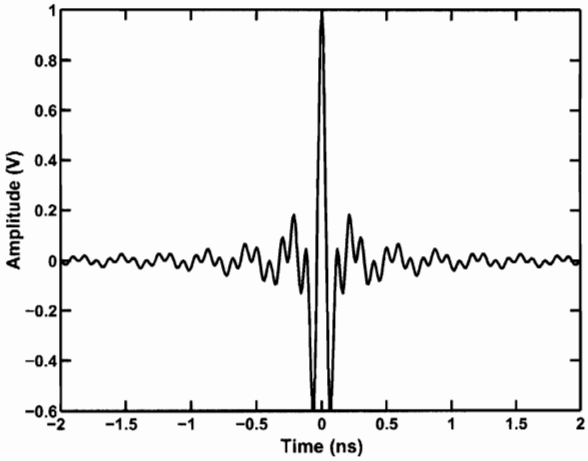

Fig. 3. The UWB transmitted signal waveform.

and the transfer function of AUT is obtained by

$$H_{AUT}(\theta,\varphi,f) = \frac{S_{21}(f)}{H_f(f,d)H_{Std}(f)}. \quad (13)$$

3.2 Measurement Setup

The VNA was operated in the response measurement mode, where Port-1 was the transmitter port (Tx) and Port-2 was the receiver port (Rx), respectively. Biconical antennas with the maximum diameter of 65.3 mm and the length of 37 mm are used both as the standard antennas and as AUT [2]. The measurement was done in the anechoic chamber. Both Tx and Rx antennas were fixed at the height of 1.75 m and separated at a distance of 3 m.

3.3 UWB Antennas

The geometry and dimensions of the antenna and its characteristics are in Ref. [2]. From Fig. 2 the largest dimension of each Tx and Rx antennas are the inclined height $D_t = D_r = 75$ mm. The largest

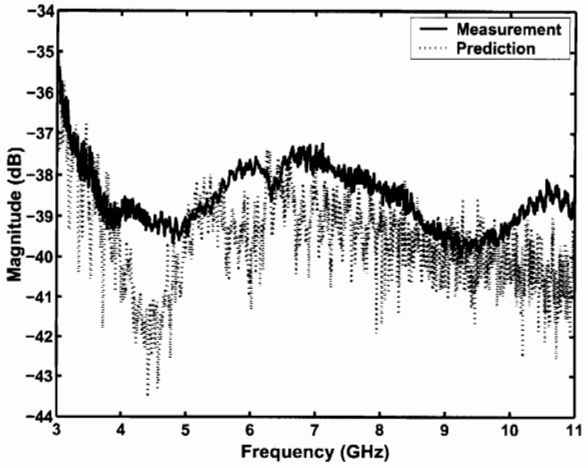

Fig. 4. The antenna transfer function at 0.3 m distances: magnitude.

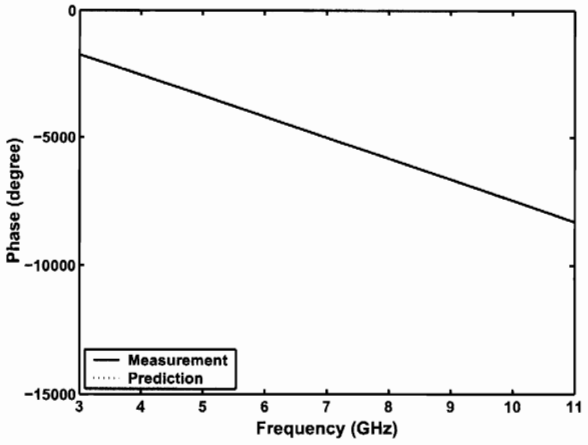

Fig. 5. The antenna transfer function at 0.3 m distances: phase.

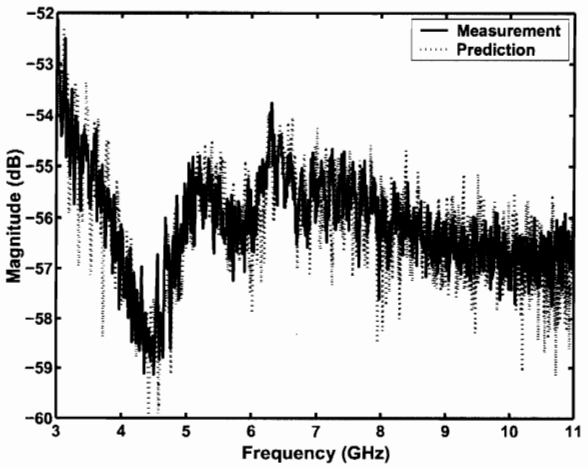

Fig. 6. The antenna transfer function at 2 m distances : magnitude.

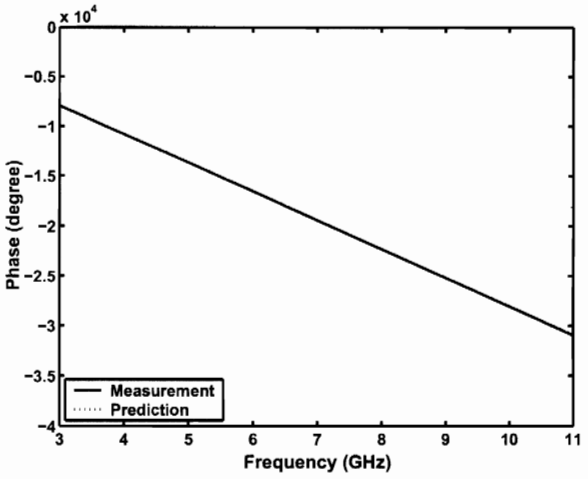

Fig. 7. The antenna transfer function at 2 m distances: phase.

dimension of the antenna considering the field regions are $D = D_t + D_r = 150$ mm. For the whole UWB frequency spectrum, the inner boundary distance of the Fresnel region is 0.21 m while the outer boundary distance is 0.47 m. The inner boundary distance of the far field region for the whole UWB frequency spectrum is 1.59 m. Then, 0.3 m TR separation distances are chosen for the Fresnel region, while 2.0 m TR separation distances are chosen for the far field region. The practical maximum measured distance, 3 m, is chosen as reference distance to estimate the accuracy of the antenna transfer function. The Tx and Rx antennas are assumed to be identical.

3.4 UWB Transmitted Signal Waveform

The effect of the waveform distortion is more obvious when the bandwidth is wider. We considered the impulse radio signal that fully covers the FCC band [4], i.e., $3.1 \sim 10.6$ GHz is used to test the distortion of the received UWB waveform. This waveform is expressed by

$$v_{\mathrm{t}}(t) = \frac{1}{f_{\mathrm{b}}}[f_{\max}\mathrm{sinc}(2f_{\max}t) - f_{\min}\mathrm{sinc}(2f_{\min}t)], \quad (14)$$

where $f_{\min} = 3.1$ GHz is the minimum frequency, $f_{\max} = 10.6$ GHz is the maxmimum frequency, $f_{\mathrm{b}} = f_{\max} - f_{\min}$ and $\mathrm{sinc}(x) = \sin(\pi x)/(\pi x)$. This signal waveform in time domain shown in Fig. 3.

4. Experiment Results

The transfer function of Tx and Rx antennas are estimated by using the channel transfer function at 4 m, assuming that these antennas are with identical transfer function. Figures 4, 5 and 6, 7 show the magnitude and the phase of the transfer functions measured at 0.3 and 2.0 m distances. In Figs. 4 and

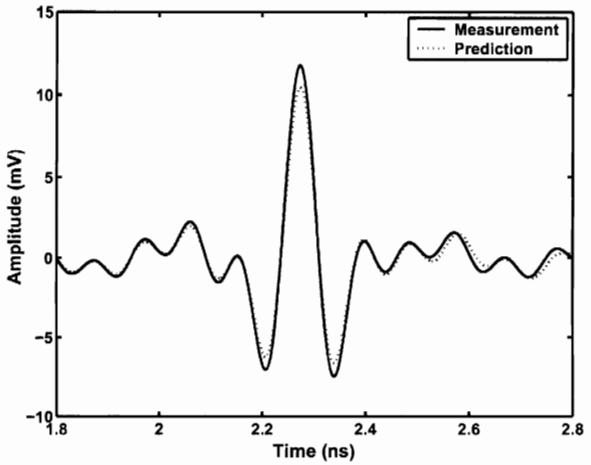

Fig. 8. The received signal waveforms at 0.3 m distances.

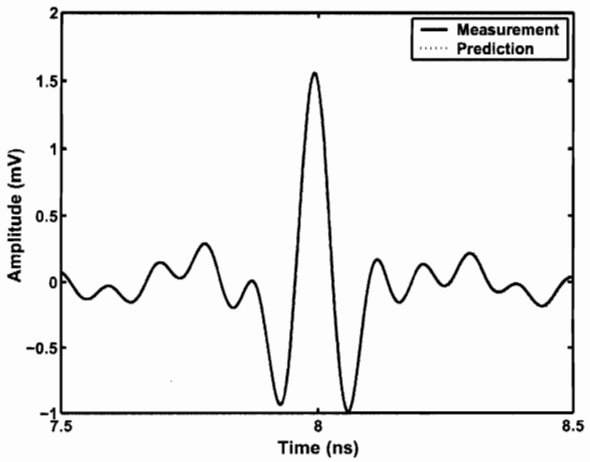

Fig. 9. The received signal waveforms at 2.0 m distances.

TABLE I Path loss of the received UWB waveform.

	Path loss	
	0.3 m (dB)	2.0 m (dB)
Measured	38.58	56.16
Prediction	39.63	53.20

TABLE II the percent of the correlation coefficient of the received UWB waveform.

	correlation coefficient	
	0.3 m (%)	2.0 m (%)
Prediction	99.45	99.94

5, the measured values are compared with the predicted and complex form Friis' transmission formula. Both results are almost identical in the far field region, but the differences of magnitude are observed in the Fresnel region. We can clearly see that in the Fresnel region, the measured magnitude results are greater than the predicted magnitude results. This is due to the radial field in the Fresnel region. In the far field region, the radial field can be negligible.

Figures 8 and 9 compares the transmission of the received UWB waveform presented in Fig. 3, by using the measured transfer functions and those predicted by using the complex form Friis' transmission formula and the antenna transfer function. We can see a little difference between the measured and the predicted waveforms in the Fresnel region. In the far field region on the other hand, the received waveforms are almost the same. Table 1 summarizes the results of Figs. 8 and 9 with respect to the path loss. As expected from Figs. 8 and 9 the difference of the path gain is more obvious in the Fresnel region. Table 2 shows the correlation between two waveforms corresponding to the measured and the predicted transfer functions. It has higher distortion in the Fresnel region. While in the far field region, the distortion is very small.

5. Conclusion

In this paper we discusses the complex form Friis' transmission formula in Fresnel region has been experimentally studied to consider the UWB free space channel model. The error of the path loss is observed in the Fresnel region caused by the radial field. More comprehensive studies are necessary to consider the type of antennas and to find how to compensate the error. This approch is more useful for design and evaluation of UWB wireless systems.

References

[1] S. Promwong, and J. Takada, "Free space link budget estimation scheme for ultra wideband impulse radio with imperfect antennas," IEICE Electronics Express, vol. 1, no. 7, pp. 188–192, July 2004.

[2] S. Promwong and W. Hachitani, and J. Takada, "Free Space Link Budget Evaluation of UWB-IR Systems," *2004 International Workshop on Ultra Wideband Systems Joint with Conference on Ultra Wideband Systems and Technology* (Joint UWBST&IWUWBS2004), to be presented, May 2004.

[3] H. T. Friis, "A Note on a Simple Transmission Formula," *Proc. IRE*, Vol 34, no 5, pp. 254-256, May 1946.

[4] Federal Communications Commission, "Revision of Part 15 of the Commission's Rules Regarding Ultra-Wideband Transmission Systems," First Report and Order, FCC 02–48, Apr. 2002.

Simple Waveforms Satisfied CEPT Radiation Limits for UWB Communications

Kritsana Wansiang[1], Pichaya Supanakoon[1], Sathaporn Promwong[1] and Junichi Takada[2]

[1]Department of Information Engineering, Faculty of Engineering,
King Mongkut's Institute of Technology Ladkrabang, Bangkok 10520, Thailand.
Email: {s7061132, kspichay, kpsathap}@kmitl.ac.th

[2]Graduate School of Science and Engineering, Tokyo Institute of Technology,
2-12-1-S6-4, O-okayama, Meguro-ku, 152-8550, Tokyo, Japan.
Email: takada@ide.titech.ac.jp

***Abstract*— In this paper, the simple waveforms are considered for satisfying the European Conference of Postal and Telecommunications (CEPT) radiation limits. The rectangular passband, modulated rectangular and modulated Gaussian waveforms are considered. They are optimized for maximum bandwidth, amplitude and average power in the frequency rage from 3.1 to 10.6 GHz. The binary pulse-amplitude modulation (PAM) with balance binary data independent identically distributed random sequence is considered to easily derive the power spectral density (PSD) of the waveforms. The power spectral density (PSD) and parameters of each optimized waveform are showed. The optimized results are discussed in the conclusion.**

I. INTRODUCTION

Recently, ultra wideband (UWB) radio technology has become an important topic for microwave communication because its potential is low cost and low power consumption properties [1]. UWB is different from other radio frequency (RF) technologies. Instead of using a narrow carrier frequency, UWB transmits pulses of power spectral density (PSD) in the range of the ultra wide frequency spectrum. The Federal Communications Commission (FCC) [2] in US defined the UWB signal as those which have a fractional bandwidth greater than 0.20 or occupies bandwidth greater than 500 MHz. The fractional and occupies bandwidth are defined as

$$\text{Fractional bandwidth} = \frac{2(f_{\mathrm{H}} - f_{\mathrm{L}})}{f_{\mathrm{H}} + f_{\mathrm{L}}}, \quad (1)$$

$$\text{Occupies bandwidth} = f_{\mathrm{H}} - f_{\mathrm{L}}, \quad (2)$$

where f_{L} and f_{H} are the lower and upper frequencies at the -10 dB point, respectively.

There are there radiation limits of the UWB signal for the indoor and outdoor applications such as FCC spectral masks and European Conference of Postal and Telecommunications (CEPT) spectral masks [3] proposed by European Telecommunications Standards Institute (ETSI). The power density of the UWB signal is considered to be noise for other communication systems because its power spectrum is below the part 15 noise limit. The UWB receiver collects the power of the received signal to rebuild the pulse. Therefore, UWB radio technology can coexist with other RF technologies without interference.

Numerous UWB waveforms have been proposed [4]. The waveform designs are reviewed, but no considered about the UWB definition and spectral limits. There are many techniques for designing the UWB waveform such as by using the Hermite function [5]-[6] and prolate spheroidal wave function [7]. The numerical technique is also used to design the UWB waveform [8]-[9]. Although the waveform has very high effective spectral in the designed frequency range, but the algorithms of these techniques are complicated. After that, the simple waveforms for UWB communications are proposed [10]. But they did not consider for the CEPT radiation limits.

In this paper, the simple waveforms are considered for satisfying the CEPT radiation limits. The CEPT indoor and outdoor masks for the UWB communications are shown in Fig. 1. The rectangular passband, modulated rectangular and modulated Gaussian waveforms are considered. They are optimized for maximum bandwidth, amplitude and average power in the frequency rage from 3.1 to 10.6 GHz. The binary pulse-amplitude modulation (PAM) with balance binary data independent identically distributed random sequence is considered to easily derive the power spectral density (PSD) of the waveforms. The power spectral density (PSD) and parameters of each optimized waveform are showed. The optimized results are discussed in the conclusion.

II. WAVEFORM MODEL

The rectangular passband, modulated rectangular and modulated Gaussian waveforms are considered. These waveforms are assumed to be voltage signals. For obtaining the continuous component of power spectral density (PSD), the binary PAM with balance binary data independent identically distributed random sequence is considered. Then, the power spectral density (PSD) of the transmitted waveform can be simplified to [9]

$$S(f) = \frac{1}{T_{\mathrm{s}}}|F(f)|^2, \quad (3)$$

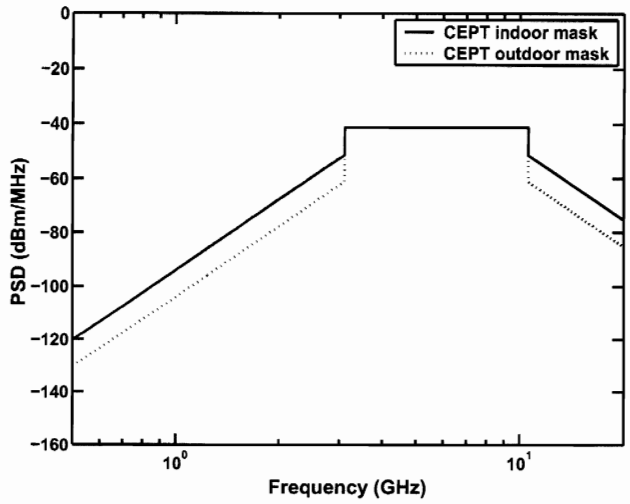

Fig. 1. CEPT indoor and outdoor masks for UWB communications.

where T_s is the time interval of one waveform and $F(f)$ is the spectral density function of the waveform. The spectral density function can be calculated by using Fourier transform,

$$F(f) = \int_{-\infty}^{\infty} f(t) e^{-j2\pi ft} dt, \tag{4}$$

where $f(t)$ is the waveform in time domain.

A. Rectangular Passband Waveform

The rectangular passband waveform in time domain and its spectral density function are given by

$$f(t) = \frac{A}{f_b}[f_H \text{sinc}(2f_H t) - f_L \text{sinc}(2f_L t)], \tag{5}$$

$$F(f) = \begin{cases} \frac{A}{2f_b} & ||f| - f_c| \le \frac{f_b}{2} \\ 0 & ||f| - f_c| > \frac{f_b}{2} \end{cases}, \tag{6}$$

where A is the maximum amplitude, f_b is the occupies bandwidth, f_c is the center frequency, $f_L = f_c - f_b/2$ and $f_H = f_c + f_b/2$ are the minimum and maximum frequencies, respectively.

This waveform has the $A/(2f_b)$ constant magnitude of spectral density in the $-f_H$ to $-f_L$ and f_L to f_H frequency ranges. The area of its spectral density is $\int_{-\infty}^{\infty} F(f)df = A$, then this waveform has maximum amplitude is A at $t = 0$. This is the ideal case of the UWB waveform then it used to considered the upper limit of the maximum bandwidth, amplitude and power for the UWB waveform.

B. Modulated Rectangular Waveform

The modulated rectangular waveform in time domain and its spectral density function are given by

$$f(t) = \begin{cases} A\sin(2\pi f_c t) & |t| \le \frac{t_b}{2} \\ 0 & |t| > \frac{t_b}{2} \end{cases}, \tag{7}$$

$$F(f) = \frac{At_b}{j2} \begin{Bmatrix} \text{sinc}[t_b(f - f_c)] \\ -\text{sinc}[t_b(f + f_c)] \end{Bmatrix}, \tag{8}$$

where A is the maximum amplitude, f_c is the carrier frequency and t_b is the pulse width of the waveform.

This waveform is modulated between the A constant amplitude and t_b width rectangular pulse and f_c carrier frequency. The sine function is used for reducing the direct current (DC) component of the modulated waveform to zero.

C. Modulated Gaussian Waveform

The modulated Gaussian waveform in time domain and its spectral density function are given by

$$f(t) = Ae^{-(t/d)^2} \sin(2\pi f_c t), \tag{9}$$

$$F(f) = \frac{Ad\sqrt{\pi}}{j2} \begin{bmatrix} e^{-\pi^2 d^2 (f - f_c)^2} \\ -e^{-\pi^2 d^2 (f + f_c)^2} \end{bmatrix}, \tag{10}$$

where A is the maximum amplitude of the envelope waveform, f_c is the carrier frequency and d is the $1/e$ characteristic decay time.

This waveform is modulated between the A maximum amplitude, d $1/e$ characteristic decay time of Gaussian pulse and f_c carrier frequency. The sine function is used for reducing the direct current (DC) component of the modulated waveform to zero same the modulated rectangular waveform.

III. OPTIMIZATION

The waveforms models is optimized for UWB communication. The UWB definition by FCC is considered [2]. The condition of f_L and f_H are set to 3.1 GHz $\le f_L < f_H \le$ 10.6 GHz. Each waveform must has fractional bandwidth greater than 0.20 or occupies bandwidth greater than 500 MHz. After that, each waveform is satisfied the CEPT radiation limits. The three assumptions for good UWB signal waveform are consider. First is high bandwidth for reducing the effect of multipath fading [10]. Next is high amplitude for increasing the efficiency of peak detection receiver. Final is high average power for increasing the signal to noise ratio (SNR). Then, each waveform is optimized for maximum bandwidth, amplitude and average power in the frequency range from 3.1 to 10.6 GHz. For the optimizations, the solution of frequency is 0.01 GHz, the time is 0.01 ns and the amplitude is 0.01 V.

A. Optimization of Rectangular Passband Waveform

For the indoor and outdoor limits, the parameters obtain from the maximum bandwidth, amplitude and average power optimizations are the same. The results are $f_b = 7.50$ GHz, $f_c = 6.85$ GHz, $f_L = 3.10$ GHz, $f_H = 10.60$ GHz and $A = 4.08\sqrt{T_s}$ V. The optimized waveform has 1.09 fractional bandwidth and 7.5 GHz occupies bandwidth. The average power of this waveform is -59.54 dBm. Its PSD compared with CEPT indoor and outdoor masks are shown in Fig. 2.

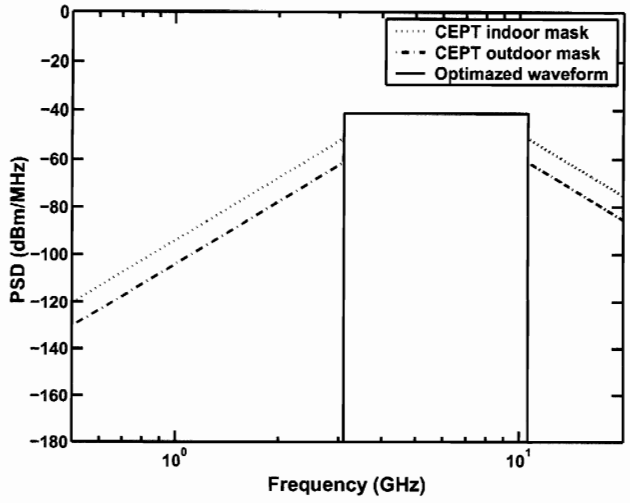

Fig. 2. PSD of optimized rectangular passband waveform compared with CEPT indoor and outdoor masks.

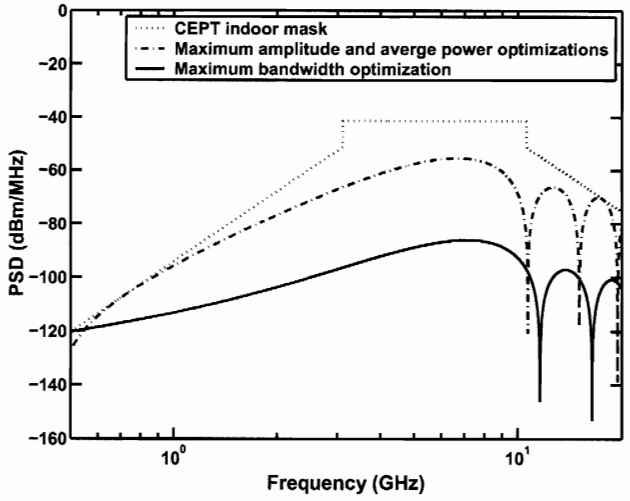

Fig. 3. PSD of optimized modulated rectangular waveform compared with CEPT indoor mask.

B. Optimization of Modulated Rectangular Waveform

For the indoor mask, the parameter obtain from the maximum bandwidth optimization are $t_{\mathrm{b}} = 0.21$ ns, $f_{\mathrm{c}} = 6.63$ GHz and $A = 0.016\sqrt{T_{\mathrm{s}}}$ V. The optimized waveform has 1.08 fractional bandwidth and 7.36 GHz occupies bandwidth. The average power of waveform is -106.67 dBm. For the maximum amplitude and average power optimizations, the parameters are the same. The obtained results are $t_{\mathrm{b}} = 0.23$ ns, $f_{\mathrm{c}} = 6.23$ GHz and $A = 0.48\sqrt{T_{\mathrm{s}}}$ V. The optimized waveform has 0.99 fractional bandwidth and 6.46 GHz occupies bandwidth. The average power of waveform is -76.50 dBm. The PSD compared with CEPT indoor mask are shown in Fig. 3.

For the outdoor mask, the parameter obtain from the maximum bandwidth optimization are $t_{\mathrm{b}} = 0.21$ ns, $f_{\mathrm{c}} = 6.63$ GHz and $A = 0.005\sqrt{T_{\mathrm{s}}}$ V. The optimized waveform has 1.08 fractional bandwidth and 7.36 GHz occupies bandwidth. The average power of waveform is -116.67 dBm. For the maximum amplitude and average power optimizations, the parameters are the same. The obtained results are $t_{\mathrm{b}} = 0.23$ ns, $f_{\mathrm{c}} = 6.23$ GHz and $A = 0.15\sqrt{T_{\mathrm{s}}}$ V. The optimized waveform has 0.99 fractional bandwidth and 6.46 GHz occupies bandwidth. The average power of waveform is -86.50 dBm. The PSD compared with CEPT outdoor mask are shown in Fig. 4.

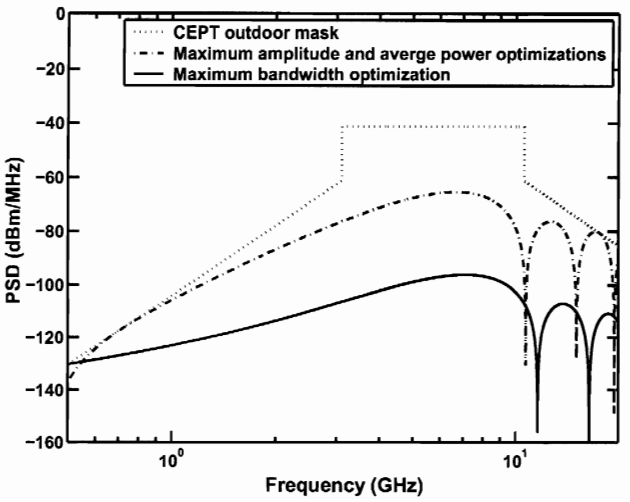

Fig. 4. PSD of optimized modulated rectangular waveform compared with CEPT outdoor mask.

C. Optimization of Modulated Gaussian Waveform

For the indoor mask, the parameters obtain from the maximum bandwidth optimization are $d = 0.10$ ns, $f_{\mathrm{c}} = 6.85$ GHz and $A = 0.025\sqrt{T_{\mathrm{s}}}$ V. The maximum amplitude is $0.022\sqrt{T_{\mathrm{s}}}$ V. The optimized waveform has 0.99 fractional bandwidth and 6.82 GHz occupies bandwidth. The average power of waveform is -104.13 dBm. For the maximum amplitude optimization the obtained results are $d = 0.13$ ns, $f_{\mathrm{c}} = 7.97$ GHz and $A = 2.36\sqrt{T_{\mathrm{s}}}$ V. The maximum amplitude is $2.23\sqrt{T_{\mathrm{s}}}$ V. The optimized waveform has 0.66 fractional bandwidth and 5.24 GHz occupies bandwidth. The average power of waveform is -63.49 dBm. For the maximum average power optimization, the obtained results are $d = 0.13$ ns, $f_{\mathrm{c}} = 7.86$ GHz and $A = 2.36\sqrt{T_{\mathrm{s}}}$ V. The maximum amplitude is $2.23\sqrt{T_{\mathrm{s}}}$ V. The optimized waveform has 0.67 fractional bandwidth and 5.24 GHz occupies bandwidth. The average power of waveform is -63.47 dBm. The PSD compared with CEPT indoor mask are shown in Fig. 5.

For the outdoor mask, the parameters obtain from the maximum bandwidth optimization are $d = 0.10$ ns, $f_{\mathrm{c}} = 6.85$ GHz and $A = 0.007\sqrt{T_{\mathrm{s}}}$ V. The maximum amplitude is $0.006\sqrt{T_{\mathrm{s}}}$ V. The optimized waveform has 0.99 fractional bandwidth and 6.82 GHz occupies bandwidth. The average power of waveform is -114.13 dBm. For the maximum amplitude optimization the obtained results are $d = 0.15$ ns,

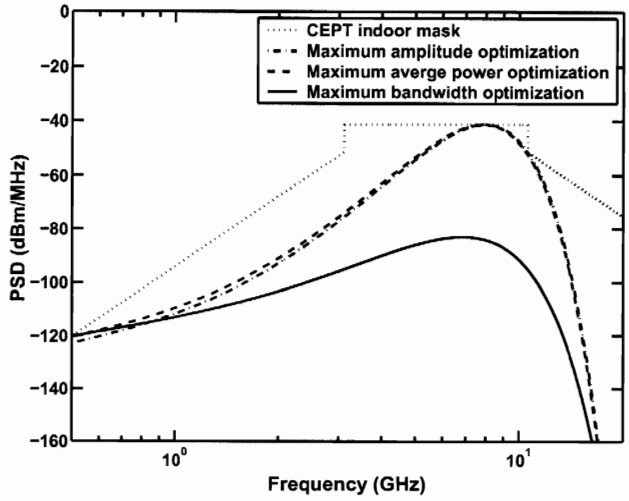

Fig. 5. PSD of optimized modulated Gaussian waveform compared with CEPT indoor mask.

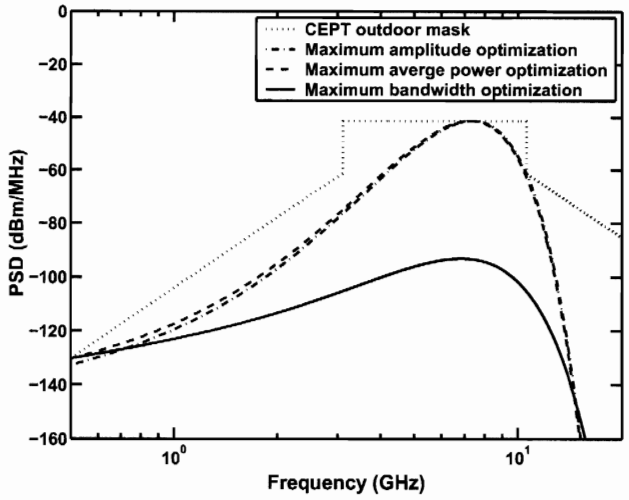

Fig. 6. PSD of optimized modulated Gaussian waveform compared with CEPT outdoor mask.

$f_c = 7.37$ GHz and $A = 2.05\sqrt{T_s}$ V. The maximum amplitude is $1.95\sqrt{T_s}$ V. The optimized waveform has 0.61 fractional bandwidth and 4.54 GHz occupies bandwidth. The average power of waveform is -64.04 dBm. For the maximum average power optimization, the obtained results are $d = 0.15$ ns, $f_c = 7.28$ GHz and $A = 2.05\sqrt{T_s}$ V. The maximum amplitude is $1.95\sqrt{T_s}$ V. The optimized waveform has 0.62 fractional bandwidth and 4.54 GHz occupies bandwidth. The average power of waveform is -64.04 dBm. The PSD compared with CEPT outdoor mask are shown in Fig. 6.

IV. CONCLUSION

In this paper, the simple waveforms are considered for satisfying the CEPT radiation indoor and outdoor limits. The rectangular passband, modulated rectangular and modulated Gaussian waveforms are considered. From the optimization results, the rectangular passband waveform obtained the maximum bandwidth, amplitude and average power. It can consider to be the upper band or the best case of UWB waveform. For the comparison between the modulated rectangular and modulated Gaussion waveform, the modulated rectangular waveform obtained the wider bandwidth for the indoor and outdoor limits. The modulated Gaussion obtain the higher amplitude for the indoor and outdoor limits.

REFERENCES

[1] K. Siwiak, "Ultra-Wide Band Radio: Introducing a New Technology," *2001 Spring IEEE Vehicular Technology Conference (VTC)*, vol. 2, pp. 1088-1093, May 2001.

[2] Federal Communications Commission, "Revision of Part 15 of the Commission's Rules Regarding UWB Transmission Systems," *First Report*, FCC 02-48, Apr. 2002.

[3] ETSI, "Harmonised Standards Covering Ultrawide Band (UWB) Applications," *Standisation Mandate: DG ENTR/G/3M/329*, Brussels, Feb. 2003.

[4] B. Allen, S. A. Ghorashi and M. Ghavami, "A Review of Pulse Design for Impulse Radio," *2004 IEE Seminar on Ultra Wideband Communications Technologies and System Design*, pp. 93-97, Jul. 2004.

[5] M. Ghavami, L. B. Miscael, R. Khono, "Hermite Function Based Orthogonal Pulses for Ultra Wideband Commuincation," *The Fourth International Symposium on Wireless Personal Multimidia Communications (WPMC)*, pp. 437-440, Sep. 2001.

[6] L. B. Michael, M. Ghavami and R. Kohno, "Multiple Pulse Generator for Ultra-Wideband Communication Using Hermite Polynomial Based Orthogonal Pulses," *2002 IEEE Conference on Ultra Wideband Systems and Techniques*, pp. 47-51, May 2002.

[7] R. Dilmaghani, M. Ghavami, B. Allen, H. Aghvami, "Novel UWB Pulse Shaping Using Prolate Spheroidal Wave Functions," *IEEE Proceedings on Personal, Indoor and Mobile Radio Communications (PIMRC)*, vol. 1, pp. 602-606, Sept. 2003.

[8] A. B. Parr, B. L. Cho and Z. Ding, "A New UWB Pulse Generator for FCC Spectral Masks," *The 57th IEEE Semiannual Vehicular Technology Conference (VTC)*, vol. 3, pp. 1664-1666, Apr. 2003.

[9] A. B. Parr, B. L. Cho, K. Wallace and Z. Ding, "A Novel Ultra-Wideband Pulse Design Algorithm," *IEEE Communications Letters*, vol. 7, no. 5, pp. 219-221, May 2003.

[10] P. Supanakoon, K. Wansiang, S. Promwong and J. Takada, "Simple Waveform for UWB Communication," *The 2005 Electrical Engineering/Electronics, Computer, Telecommunications, and Information Technology International Conference (ECTI-CON 2005)*, pp. 626-629, May 2005.

IC EMC 2005

Final Call for Papers
The 2nd International Conference on
Electromagnetic Compatibility
ICEMC'05

Kata Beach Resort, Phuket, Thailand
July 27-29, 2005

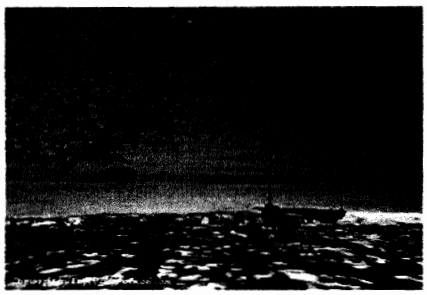

Phuket, Thailand

The 2nd international Conference on Electromagnetic Compatibility will be held in Phuket, Thailand from, July 27 - 29, 2005.

For the first time, ICEMC'05 takes place in Phuket which has been selected to host ICEMC not only because of its beautiful location but also because of its green and clean environment for you and electromagnetic.
Thus come and join ICEMC'05 in Phuket, Thailand.
We will follow world class traditional and offer you a rich scientific program of high quality with invited speakers from all over the world. As in the past, we will provide a broad forum of exchange both for academia and industry alike.
The conference will cover the entire scope of electromagnetic compatibility. Prospective authors are invited to submit original papers on their latest research results. We also solicit proposals for Topical Meetings and Tutorials.

Important Dates

Extended Summary	: April 25, 2005
Acceptance Notification	: May 25, 2005
Final Manuscript	: June 20, 2005
Conference Date	: July 27-29, 2005

All submissions must be in electronics,
No hardcopies accepted.
Details on the conference website:
www.kmitl.ac.th/emc

More information please contact:
Dr. Werachet Khan-ngern
E-mail: emc@kmitl.ac.th, icemc2005@yahoo.com, kkveerac@kmitl.ac.th

Advisory Committee

Prof. Dr. Shuichi Nitta, Salesian polytechnics, Japan
Prof. Gao Yougang, UPT, China
Prof. Dr. Todd H. Hubing, UMR, USA
Prof. Dr. Flavio Canavero, Politecnico di Torino, Italy
Prof. Dr. Gabriel Gaus, Hannover University, Germany
Prof. Dr. Christos Christopoulos, Nottingham University, UK
Prof. Dr. See Kye Yak, NTU, Singapore
Prof. Dr. Masaaki Kando, Tokai University, Japan
Mr. Heinrich A. Kunz, Schaffner, Switzerland
Prof. Dr. Osamu Fujiwara, NIT, Japan
Mr. Yukio Yamanaka, NICT, Japan
Prof. Dr. Youji Kotsuka, Tokai University, Japan
Prof. Dr. Jeong-Ki Pack, Chungnam National University, Korea
Dr. Artnarong Thansandote, Health Canda, Canada
Assoc. Prof. Dr. Tawil Pungma, KMITL, Thailand
Prof. Dr. Monai Krairiksh, KMITL, Thailand
Assoc. Prof. Dr. Samruay Sangkasaad, Thailand
Assoc. Prof. Dr. Akachai Sang-in, CMU, Thailand
Assoc. Prof. Dr. Narong Yoothanom, SPU, Thailand
Dr. Pansak Siriruchatapong, NECTEC, Thailand

Organizing Committee

Conference Chairman

Assoc. Prof. Dr. Werachet Khan-ngern, KMITL, Thailand

Technical Program Chairman

Assoc. Prof. Dr. Werachet Khan-ngern, KMITL, Thailand

Secretary

Dr. Wongwit Senawong, KMITL, Thailand.

Mr.Vuttipon Tarateeraseth, SWU, Thailand

Special Session and Exhibition

Dr. Kaison Aunchaleevarapan, PTEC, Thailand

Dr. Somyot Kaitwanidvilai, NU, Thailand

Local arrangement

Dr. Phanumas Khumsat, PSU, Thailand

EMC ReCCIT KMITL

IEEE CAS Society Thailand Chapter

IEEE THAILAND CHAPTER